ELSEVIER

Biophysical Chemistry 119 (2006) 121 – 126

Biophysical Chemistry

http://www.elsevier.com/locate/biophyschem

Lipophilic porphyrin microparticles induced by AOT reverse micelles A fluorescence lifetime imaging study

Denisio M. Togashi [a,1], Sílvia M.B. Costa [a,*], Abílio J.F.N. Sobral [b]

[a] *Centro de Química Estrutural, Complexo I-Instituto Superior Técnico, 1049-001 Lisboa, Portugal*
[b] *Departamento de Química FCTUC-Universidade de Coimbra, 3004-535 Coimbra, Portugal*

Received 28 June 2005; received in revised form 16 August 2005; accepted 17 August 2005
Available online 12 September 2005

Abstract

Fluorescence Lifetime Imaging Microscopy (FLIM) technique was applied to investigate the fluorescence dynamics and structural features of large colloidal aggregates of *meso*-tetra(*N*-dodecyl-4-amino sulfonyl-phenyl)porphyrin (PC_{12}) induced by Sodium 1,4-bis(2-ethyl hexyl)sulfosuccinate (AOT) reverse micelles. The aggregate's particle sizes (down to 1 μm) obtained from the confocal fluorescence images matched with the particle sizes measured in the images obtained from Scanning Electron Microscopy (SEM). The fluorescence decays for those aggregates in the micro spatial domain show triexponential fluorescence lifetimes ($\tau_1 \sim 12$ ns, $\tau_2 \sim 3$ ns and $\tau_3 \sim 1$ ns) which are independent of the aggregate's size.

Keywords: Fluorescent particles; Fluorescence lifetime imaging; Aggregation; Porphyrin

1. Introduction

Enzymes and carrier proteins essential for several functions in living organisms contain porphyrins as prosthetic groups. The observation that these dyes accumulate selectively in tumours cells has attracted a special interest in porphyrin derivatives for therapeutic applications [1]. Such accumulation depends on the porphyrin amphiphilic structure which in turn can affect the degree of porphyrin self-aggregation. The great ability of this class of molecules to form aggregates has been intensively investigated in many fields [2–6]. Nano or microparticles composed of porphyrins are expected to have unique photonic properties not achieved with larger-scaled material.

Luminescent particles can be formed when a fluorescent dye is incorporated either covalently linked to or adsorbed on a solid matrix (latex spheres, silica particles, etc.) [7–9]. In the colloidal field, these particles can have particular relevance for many technological and biotechnological applications such as fluorescence microspheres used as markers for cellular antigens [10,11], flow cytometry [12] or for rheological evaluation [13].

Water-in-oil reverse micelles are large, thermodynamically stable aggregates formed with amphiphilic molecules in an oil pseudo-phase with their polar heads pointing inward towards the polar pool (Scheme 1). They have been used as microreactors for different chemical reactions that are largely affected by the restricted geometry and by the properties of the water molecules in the interfacial region and as mimetics for lipid–protein interfaces. These systems are usually correlated with the water to surfactant molar ratio (ω_0=[water]/[surfactant]) [14] and can be useful to act as templates for the formation and size control of nanoparticles and microparticles [15–17].

Recently, we reported fluorescent aggregates of *meso*-tetra(*N*-dodecyl-4-amino sulfonylphenyl)porphyrin (PC_{12}) formed in Sodium 1,4-bis(2-ethylhexyl) sulfosuccinate (AOT) reverse micelles and/or micelles [18]. PC_{12} is incorporated as a monomer species in large concentration of reverse micelles, which can be achieved with low concentrations of dissolved water (see structures in Scheme 1). By contrast, the aggregation phenomenon is observed when the micellar concentration is reduced, increasing the water concentration at constant AOT

* Corresponding author. Tel.: +351 218419271; fax: +351 21 846 4455/7.
E-mail address: sbcosta@mail.ist.utl.pt (S.M.B. Costa).
[1] Present address: National Centre for Biomedical Engineering Science, National University of Ireland, Galway, Ireland.

0301-4622/$ - see front matter © 2005 Elsevier B.V. All rights reserved.
doi:10.1016/j.bpc.2005.08.005

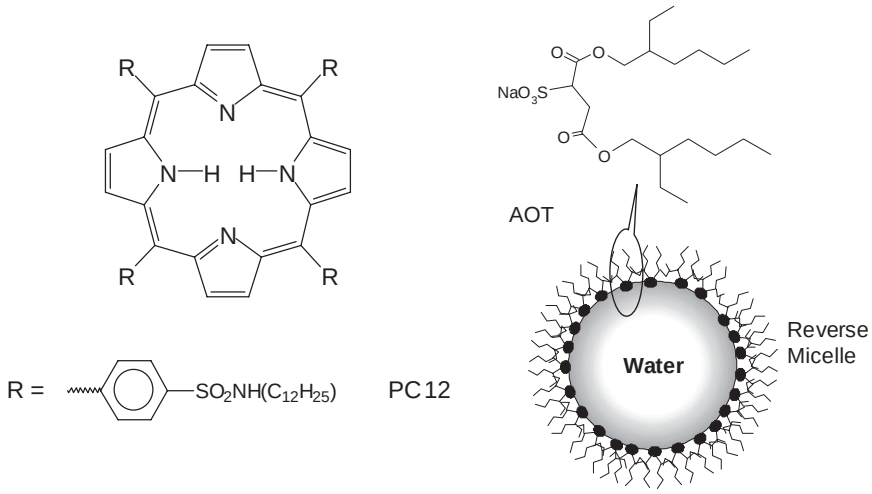

Scheme 1.

concentration (0.1 M). In addition, the resonance light scattering (RLS) results showed that large aggregates of colloidal size are present when considerable amounts of water are dissolved in the system. It was observed that such aggregates of colloidal size do fluoresce.

Confocal Fluorescence Microscopy can be used to determine the position and structure of fluorescent species at submicrometer resolution that is restricted by the diffraction limit of excitation light. Fluorescence lifetime imaging (FLIM) is the technique that measures the fluorescence decays at submicrometer spatial resolution of an entire observed region. Besides the image contrast, FLIM results provide fluorescence lifetimes which depend on the photophysics of fluorophore and the physico-chemical properties of the surrounding medium, such as viscosity, pH, polarity, and interaction with other molecules [19].

In this work we report novel results which show that particles formed by porphyrin homo-aggregation induced by reversed micelles are indeed fluorescent species. In addition, these particles can be excited at long wavelength (>635 nm) while the majority of reported fluorescent particles are excited at shorter wavelength. Fluorescence particles with long excitation and emission wavelengths have been described only recently, but they were still formed by a dye incorporated into a polymeric matrix [7]. In order to demonstrate that the particles are fluorescent species formed by porphyrin aggregates with micrometer controllable size, we used the confocal fluorescence microscopy, confocal fluorescence lifetime imaging (FLIM), charge coupled device (CCD) camera images and scanning electron microscopy (SEM) of such large aggregates in the micro-spatial domain.

2. Experimental section

2.1. Materials

The porphyrin PC_{12} (Scheme 1) was synthesized and purified as already described [20]. The AOT and all organic solvents (chloroform and isooctane) were purchased from Sigma-Aldrich and used without any further treatment. The water used was previously doubly distilled.

2.2. Apparatus

The decay time and the Fluorescence Lifetime Imaging were obtained using the Microtime 200, from Picoquant GmbH (Berlin, Germany) (Scheme 2). The instrument setup includes the inverse microscope (Olympus IX 71) with ×20, ×40 and ×100 objectives. A permanent online analysis of the backreflected and backscattered excitation light is achieved with a CCD camera which monitors the image seen by the objective. The sample holder is positioned on a XY stage E-710 Digital PZT Controller with scanning range of 100 × 100 μm^2 with 1 nm resolution. The image resolution is 50 nm per pixel. The measurements were performed using 638 nm (20 MHz, 0.6 mW, 83 ps) excitation wavelength with the band-pass 695/55 emission filter placed in front of photomultiplier

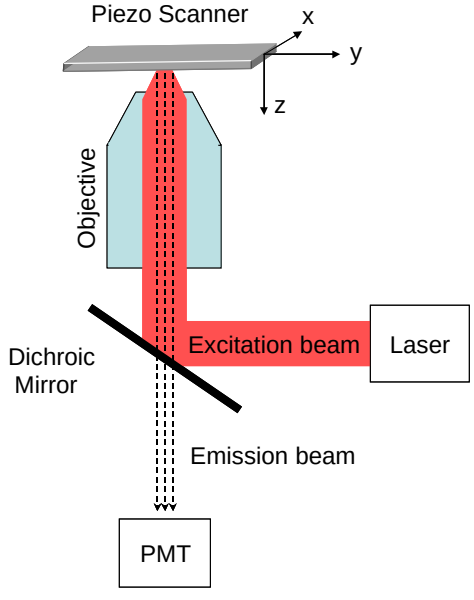

Scheme 2.

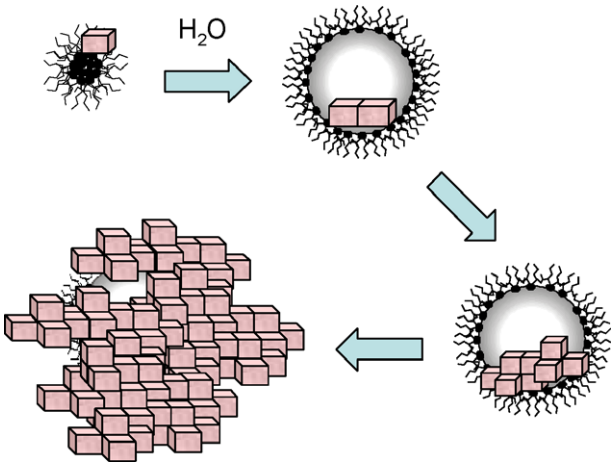

Scheme 3.

tube from Picoquant (model PMA-182). Data acquisition is performed in a PC equipped with Timeharp 200 TCSPC board, Picoquant. A more detailed description of the instrument is found elsewhere [21]. Scanning electron microscopy (SEM) measurements were performed in a Field Emission SEM Hitachi S4100.

2.3. Fluorescence lifetime imaging

The imaging process obtained from the Microtime 200 equipment is dependent on the decay fit from the sample. Firstly, the fluorescence intensity image is obtained and then total intensity decay is built by a sum of all individual decays per pixel. The decay times are obtained by fitting the total image decay from a multiexponential function model (Eq. (1)).

$$I(t) = \sum_i A_i \exp(-t/\tau_i). \quad (1)$$

The A_i values are the amplitudes to the corresponding decay time τ_i. From the decay times values, the FLIM are now performed recalculating the amplitudes per each pixel with decay times fixed. Finally, colors are assigned to each decay times and brightness to the amplitudes. The intensity fraction is calculated from Eq. (2):

$$f_i = A_i\tau_i \Big/ \sum_j A_j\tau_j \quad (2)$$

The microscopic images were then obtained from the multiexponential fittings which were performed excluding the instrumental response function convolution. The fittings were started with a delay after approximately 300 ps (laser width at half maximum) from the laser pulse peak.

2.4. Sample preparation

For the preparation of isooctane/AOT/water reverse micelles, 0.1 Molar of AOT was used. Appropriate volumes from a PC_{12} chloroform stock solution were added to an empty volumetric flask and then the solvent carefully evaporated using a dry nitrogen flow. Then, the porphyrin thin films formed in the bottom wall of the flask were dissolved with the addition of isooctane/AOT solution. This solution ($\omega_0=0$) was then filtered through PVDF Durapore membrane (0.45 μm) from Millex Millipore. PC_{12} was around 3×10^{-6} M of

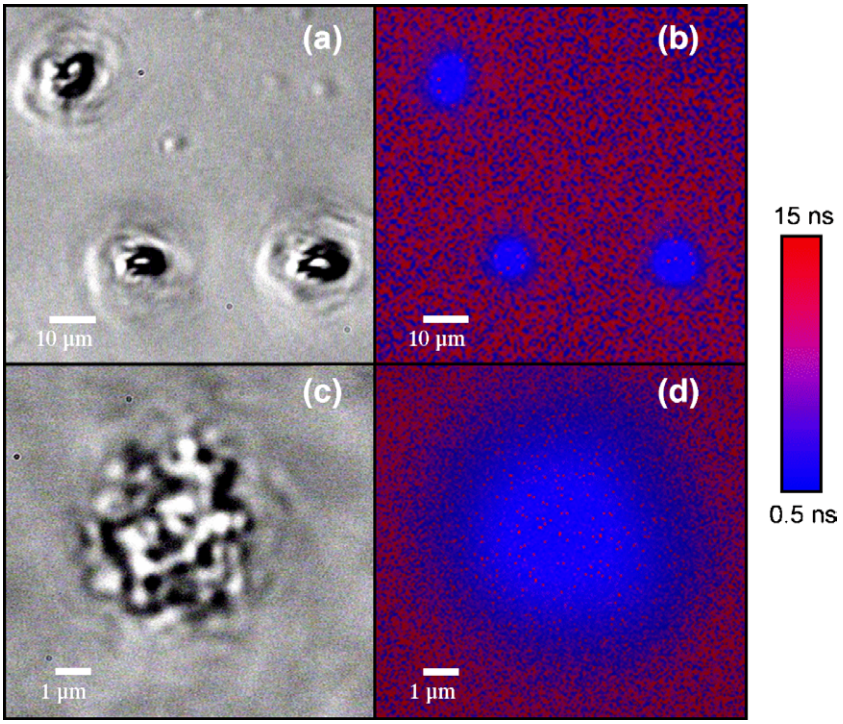

Fig. 1. Images of PC_{12} particles in AOT films spread on the cover slip prepared from $\omega_0=10$ solution. (a) CCD picture of three particles. (b) Fluorescence lifetime image for the particles at the same position in (a). The Figures (c) and (d) are zoom regions for the pictures (a) and (b), respectively.

Table 1
FLIM fitting parameters

ω_0	τ_1 (ns)	τ_2 (ns)	τ_3 (ns)	f_1	f_2	f_3
0	11.8±0.4	3.3±0.7	–	0.91±0.02	0.09±0.02	–
10	12.9±2.1	2.6±0.4	1.2±0.3	0.25±0.21	0.33±0.10	0.41±0.16
20	12.0±0.3	2.7±0.7	0.9±0.1	0.58±0.21	0.17±0.08	0.27±0.15
40	12.1±0.5	3.1±1.0	0.8±0.2	0.73±0.15	0.12±0.05	0.15±0.14

Parameters are averages of large images obtained from each sample. χ^2 for ω_0=0, 10, 20 and 40 are 1.048, 1.045, 1.034 and 1.043, respectively.

concentration. The reverse micelles at different molar ratios, ω_0 were prepared by addition of corresponding water volumes to the solution of AOT in isooctane with the porphyrin already incorporated. The solutions were stirred until total transparency was observed and then left overnight at room temperature before carrying out any measurements. The sample preparation for the microscopic imaging studies used the corresponding solution of the microparticles and approximately 50 μl was spread on the glass cover slips (20 mm × 20 mm) with 0.17 mm of thickness and then the solvent evaporated. Afterwards, the glass cover slips were kept in desiccators at 10^{-3} Torr and at room temperature during one day.

3. Results and discussion

PC_{12} is a porphyrin grafted with four lipophilic long alkyl chains which helps to dissolve the molecule in organic apolar solvents. However, PC_{12} is insoluble in hydrocarbon solvents (as isooctane) likely due to the presence of highly polar aminosulfonyl groups. In the presence of an anionic surfactant such as AOT, at the concentration needed for reverse micelles formation, the porphyrin is solubilized in isooctane due to the hydrophobic interactions between the porphyrin and micelles. PC_{12} is dissolved as monomeric species. The AOT reverse micelles in the system–PC_{12}/AOT/isooctane–can solubilize water and originate a "pool" in the inner core of reverse micelles (Scheme 3). A co-effect of water solubilization in reverse micelles is the reduction of reverse micelles concentration because more surfactant molecules are needed to account for the increase of superficial area created by the water pool. Therefore, the addition of water causes indirectly the increase of local concentration of PC_{12} per reverse micelle and initiates the aggregation process of this porphyrin (Scheme 3). This process with size increase can be followed by the signals of scattering light, as previously observed by the resonance light scattering (RLS) results [18]. After reaching the equilibrium, the porphyrin particles start to sediment. On Fig. 1 are collected images of PC_{12} particles deposited from ω_0=10 (i.e., [water]=1 M) solution observed in the optical microscope. Fig. 1a and c show images of particles obtained from CCD camera coupled to the inverted microscope. The size of the particles in the image can achieve, approximately, 10 μm. Fig. 1b and d illustrate the fluorescence decay time images observed when the sample area was positioned as in Fig. 1a. It is clear that such particles fluoresce and that they are the main sources of fluorescence in the image.

Briefly, FLIM is a recent technique whereby the fluorescence intensity of whole image is followed in space (piezo scan table) and time (time-correlated single photon counting) domains; then the analysis of fluorescence decays by a multiexponential model provide decay times values that will be applied in next stage to map the image according to the decay time values, i.e., providing the fluorescence lifetime

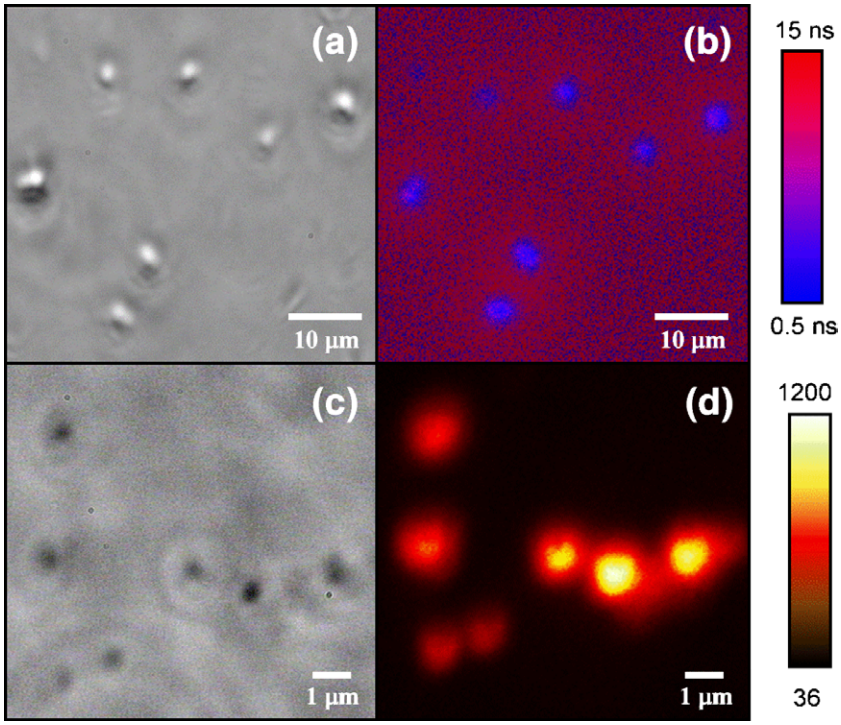

Fig. 2. CCD images of PC_{12} particles in AOT films prepared from ω_0=20 (a) and ω_0=40 (c) solutions. FLIM for ω_0=20 particles is shown in (b) and the fluorescence intensity image for ω_0=40 particles in (d) where the scale (rhs) is shown as counts per pixel.

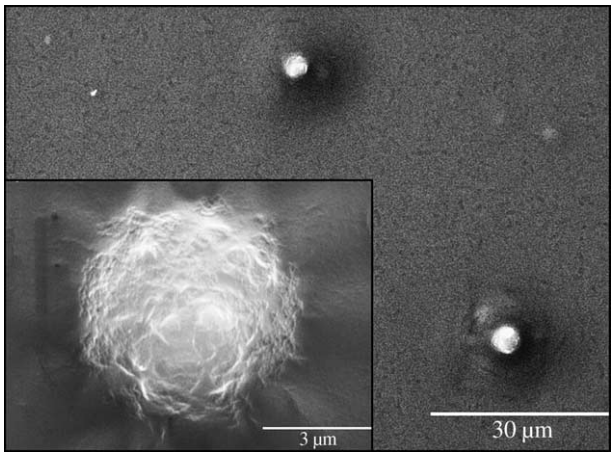

Fig. 3. SEM images of PC_{12} particles in AOT films prepared from $\omega_0=10$ solution.

imaging (FLIM). The fluorescence lifetimes obtained by this procedure must then be collated to compose the fluorescence microscopic image which is the aim of the FLIM technique.

The FLIM analysis from the fluorescence decays per pixel shows a non-exponential behavior represented by a sum of three exponentials (see Table 1). The FLIM for the $\omega_0=0$ sample shows a biexponential fluorescence decay per pixel. The parameters adjusted from the decays show mainly a long decay time component of approximately 12 ns. PC_{12} fluorescence lifetime in $\omega_0=0$ solution is 10.6 ns, and then we believe that the long decay time can be assigned to PC_{12} dispersed as a monomer. The decay time for other ω_0 values are doubtful due to the decay profile deformation whenever a particle crosses the laser beam focus. An intensification of a short component on decay profile is always observed in such case. By contrast, the short component of approximately 3 ns may be due to the small aggregates or from dynamic processes that involve energy transfer between monomers. These two decay time components also appear in samples studied with high ω_0. However, the weight of the long component in the fluorescence decays is fully dependent on the area where the image is obtained. In $\omega_0=10$, the FLIM decays in Fig. 1d show a smaller contribution to the long decay time component than the FLIM decays in Fig. 1b. Consequently, a greater number of images of large size and at different locations were obtained to give some statistical meaning and an average was made of all the fitting parameters of the imaging fluorescence decays as shown in Table 1. The particles' short decay time values (~1 ns and ~3 ns) can be due to many processes occurring when the particles are excited, such as energy transfer that involves the surroundings, the proximity of the particles themselves and the laser energy intensity dependence. Nevertheless, the presence of fluorescent particles causes a significant shortening of the imaging fluorescence decays.

Different particle sizes are observed with deposition from different micelles (Fig. 2). The results indicate that the particle's size on the spread film decreases when they are produced from micellar solutions of high ω_0. The CCD images of films formed from $\omega_0=20$ and $\omega_0=40$ solutions are not as well defined as those observed for $\omega_0=10$ films. However, it is still clear that they correspond to fluorescent species with sizes smaller than 1 μm. The accurate determination of particle sizes from fluorescence images is difficult due to the focus and the non-homogeneous thickness of the spread films. The short

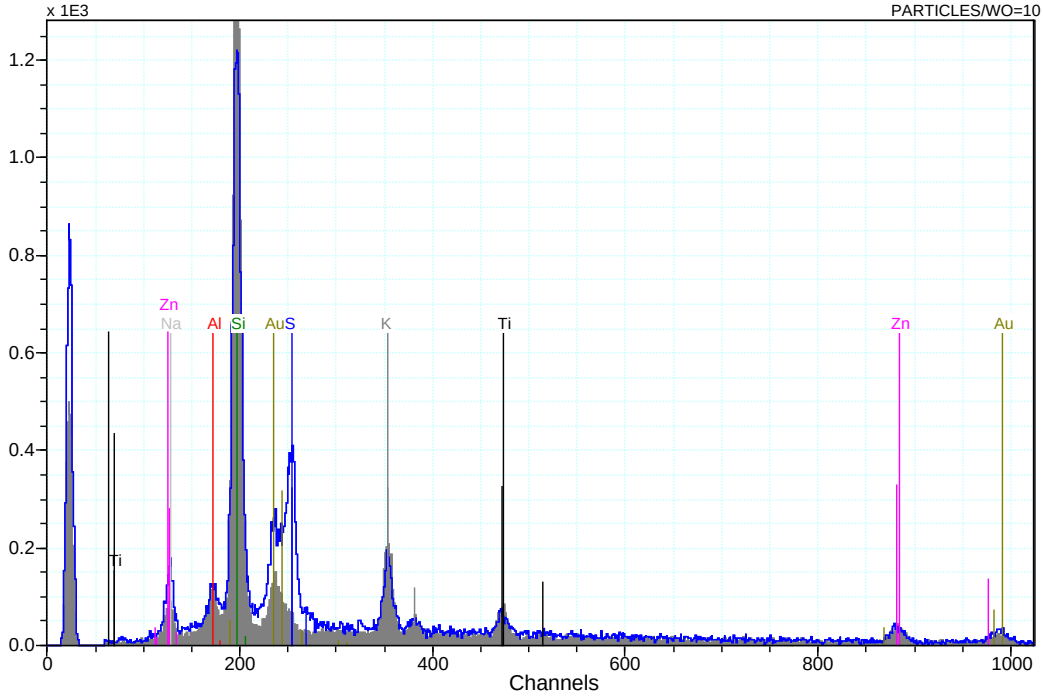

Fig. 4. Electron dispersion Spectra of PC_{12} porphyrin particles at [AOT]/[water]=10. Blue line is the Particle spectrum and the gray highlighted area the surrounding far from the particle (blank).

decay time's contributions decrease with increased ω_0 (Table 1) and, thus, the fluorescence contribution over the total area for small particles will be less. Nevertheless, the qualitative size difference observed for particles formed from ω_0=10, 20 and 40 reverse micelles is clearly visible (Figs. 1 and 2).

In previous work we have found that no significant difference is observed in the fluorescence quantum yield and the RLS signal for micellar solutions above ω_0=8. It is possible that the particles formed at higher ω_0 solutions are weakly associated in comparison to the particles formed in ω_0=10 and, thus, will break into small units on the glass slide.

The self-association observed for different ω_0 should be related to the dynamics of particle formation. The aggregates are strongly dependent on the porphyrin concentration and ω_0, the rate of particle formation increases from ω_0=10 to ω_0=40 [18]. However, if the particle induced by reverse micelles with ω_0=10 has low enough growth rate, the non-covalent hydrophobic interactions with the surfactant are more firmly established and finally a more stable structure is obtained. At higher ω_0 values, a faster growth would lead to a less cohesive structure easier to break into similar small particles. Therefore, we believe that the particle size is kinetically controlled.

The scanning electronic microscopy images obtained show particles with almost spherical symmetry containing some irregularities on the surface (Fig. 3). Comparing the CCD image (Fig. 1c) with the zoomed SEM image, for ω_0=10, the particle morphology looks like clusters of small spheres (or "grape clusters"). Unfortunately, the SEM picture does not clearly show this either because there is an excessive amount of gold on the sample deposition or due to remaining AOT thin film covering the particles (the films were not stable under excessive exposure from of the electron beam). The particles were characterized by electron dispersion spectroscopy where the presence of sulphur was detected (Fig. 4). Since the porphyrins are sulphur based compounds, this confirms the presence of PC_{12} in the particles' composition.

4. Conclusion

Fluorescent particles of size greater than 1 μm are observed in the films obtained from the PC_{12}/AOT micelle solutions. The fluorescence lifetimes of particles contained in the observed films deposited show non-exponential behavior. The particles are responsible for the short fluorescence lifetime values considerably smaller than the monomer lifetime value. Also, the particle size is dependent on the ω_0 value of the solution from which they were formed, and it is likely that the size parameter is kinetically controlled.

Acknowledgment

This work was supported by CQE4/FCT. DMT thanks FCT for the award of BPD5739/2001.

References

[1] I.J. Macdonald, T.J. Dongherty, Basic principles of photodynamic therapy, J. Porphyr. Phthalocyanines 5 (2001) 105–129.
[2] X. Gong, T. Milic, C. Xu, J.D. Batteas, C.M. Drain, Preparation and characterization of porphyrin nanoparticles, J. Am. Chem. Soc. 124 (2002) 14290.
[3] G. Li, W. Fudickar, M. Skupin, A. Klyszcz, C. Draeger, M. Lauer, J.-H. Fuhrhop, Rigid lipid membranes and nanometer clefts: motifs for the creation of molecular landscapes, Angew. Chem. Int. Ed. 41 (2002) 1828–1852.
[4] L.M. Scolaro, A. Romeo, R.F. Pasternack, Tuning porphyrin/DNA supramolecular assemblies by competitive binding, J. Am. Chem. Soc. 126 (2004) 7178–7179.
[5] K. Kano, K. Fukuda, H. Wakami, R. Nishiyabu, R.F. Pasternack, Factors influencing self-aggregation tendencies of cationic porphyrins in aqueous solution, J. Am. Chem. Soc. 122 (2000) 7494–7502.
[6] R.F. Pasternack, A. Giannetto, P. Pagano, E.J. Gibbs, Self-assembly of porphyrins on nucleic-acids and polypeptides, J. Am. Chem. Soc. 113 (1991) 7799–7800.
[7] H. Hu, R.G. Larson, Preparation of fluorescent particles with long excitation and emission wavelengths dispersible in organic solvents, Langmuir 20 (2004) 7436–7443.
[8] W. Yang, D. Trau, R. Renneberg, N.T. Yu, F. Caruso, Layer-by-layer construction of novel biofunctional fluorescent microparticles for immunoassay applications, J. Colloid Interface Sci. 18 (2001) 8204–8208.
[9] V.L. Singer, R.P. Haugland, Fluorescent labeling using microparticles with controllable stokes shift, US 5 (1996) 573, 909.
[10] H. Kimura, M. Kato, M. Ikeda, A. Nagai, Y. Okada, S. Naito, S. Oshima, K. Taniguchi, K. Kozawa, A. Morikawa, Sulfonated human immunoglobulin enhances CD16-linked CD11b expression on human neutrophils, Cell Biol. Inter. 27 (2003) 913–919.
[11] R.S. Molday, W.J. Dreyer, A. Rembaum, S.P. Yen, New immunolatex spheres–visual markers of antigens on lymphocytes for scanning electron-microscopy, J. Cell Biol. 64 (1975) 75–88.
[12] T. Horsburgh, S. Martin, A.J. Robson, The application of flow cytometry to histocompatibility testing, Transplant. Immunol. 8 (2000) 3–15.
[13] K. Edsman, J. Carlfors, R. Peterson, Rheological evaluation of poloxamer as an in situ gel for ophthalmic use, Eur. J. Pharm. Sci. 6 (1998) 105–112.
[14] P.L. Luisi, M. Giomini, M.P. Pileni, B.H. Robinson, Reverse micelles as hosts for proteins and small molecules, Biochim. Biophys. Acta 947 (1988) 209–246.
[15] J.H. Clint, I.R. Collins, J.A. Williams, B.H. Robinson, T.F. Towey, P. Cajean, A. Khan-Lodhi, Synthesis and characterization of colloidal metal and semiconductor particles prepared in microemulsions, Faraday Discuss. 95 (1993) 219.
[16] M.P. Pilleni, Fabrication and properties of nanosized material made by using colloidal assemblies as templates, Cryst. Res. Technol. 33 (1998) 1155–1186.
[17] M.A. Castriciano, A. Romeo, V. Villari, N. Micali, L.M. Scolaro, Nanosized porphyrin J-aggregates in water/AOT/decane microemulsions, J. Phys. Chem., B 108 (2004) 9054–9059.
[18] D.M. Togashi, S.M.B. Costa, A.J.F.N. Sobral, A.M.D.R. Gonsalves, Self-aggregation of lipophilic porphyrins in reverse micelles of aerosol OT, J. Phys. Chem., B 108 (2004) 11344–11356.
[19] K. Suhling, P.M.W. French, D. Phillips, Time-resolved fluorescence microscopy, Photochem. Photobiol. Sci. 4 (2005) 13–22.
[20] A.J. Hudson, T. Richardson, J.P. Thirtle, G. Roberts, R.A.W. Johnstone, A.J.F.N. Sobral, Characterization and langmuir–blodgett deposition of novel porphyrin compounds, Mol. Cryst. Liq. Cryst. 235 (1993) 103.
[21] P.M.R. Paulo, R. Gronheid, F.C. De Schryver, S.M.B. Costa, Porphyrin-dendrimer assemblies studied by electronic absorption spectra and time-resolved fluorescence, Macromolecules 36 (2003) 9135–9144.